

Results from a Prototype Chicane-Based Energy Spectrometer for a Linear Collider

A. Lyapin^{a,*}, H.J. Schreiber^b, M. Viti^b, C. Adolphsen^c, R. Arnold^c,
S. Boogert^d, G. Boorman^d, F. Gournaris^a, V. Duginov^e, C. Hast^c,
M. Hildreth^g, C. Hlaing^h, F. Jacksonⁱ, O. Khainovsky^h, Y. Kolomensky^h,
S. Kostromin^e, B. Maiheu^a, D. McCormick^c, D. J. Miller^a, N. Morozov^e,
T. Orimoto^{h,j}, M. Slater^f, Z. Szalata^c, M. Thomson^f, D. Ward^f, M. Wing^a,
M. Woods^c

^aUniversity College London, London, UK

^bDeutsches Elektronen Synchrotron DESY Hamburg and Zeuthen, Germany

^cSLAC National Accelerator Laboratory, Menlo Park, California, USA

^dRoyal Holloway, University of London, Egham, UK

^eJoint Institute for Nuclear Research, Dubna, Moscow Region, Russia

^fUniversity of Cambridge, Cambridge, UK

^gUniversity of Notre Dame, Notre Dame, Indiana, USA

^hUniversity of California and Lawrence Berkeley National Laboratory, Berkeley,
California, USA

ⁱDaresbury Laboratory, Daresbury, UK

^jCalifornia Institute of Technology, Pasadena, California, USA

Abstract

The International Linear Collider and other proposed high energy e^+e^- machines aim to measure with unprecedented precision Standard Model quantities and new, not yet discovered phenomena. One of the main requirements for achieving this goal is a measurement of the incident beam energy with an uncertainty of 10^{-4} or less. This article presents the analysis of data from a prototype energy spectrometer commissioned in 2006-2007 in SLAC's End Station A beamline. The prototype was a 4-magnet chicane equipped with beam position monitors restoring the beam orbit through the chicane. An energy resolution close to $5 \cdot 10^{-4}$ was estimated, which, however, needs to be improved for a linear collider. We also report on the operational experience with the chicane-based spectrometer and suggest ways of improving its performance.

Keywords: Energy measurement, Energy Spectrometer, Cavity Beam

*Corresponding Author, HEP Group, University College London, Gower Street, WC1E 6BT, London, United Kingdom. Tel: +44 (0)20 7679 3454; Fax: +44 (0)20 7679 7145.

Email address: al@hep.ucl.ac.uk (A. Lyapin)

¹This work was supported by the Commission of the European Communities under the 6th Framework Programme "Structuring the European Research Arm," contract number RIDS-011899 and by the Science and Technology Facilities Council (STFC)

²This work was supported by the U.S. Department of Energy under contract DE-AC02-76SF00515

³This work was supported by the U.S. Department of Energy under contract DE-FG02-03ER41279

36 1. Introduction

37 The physics potential of the next TeV-energy Linear Collider depends
38 greatly on precision energy measurements of the electron and positron beams
39 at the interaction point (IP). Such measurements are mandatory in order to
40 determine particle masses in high-rate processes. For example, measuring
41 the top mass from a threshold scan to order of 100 MeV or measuring the
42 Standard Model Higgs in direct reconstruction to about 50 MeV requires
43 knowledge of the luminosity-weighted mean collision energy to a level of
44 $1-2\cdot 10^{-4}$ to avoid center-of-mass energy (\sqrt{s}) uncertainties from dominating
45 the experimental results. Incoming beam energy (E_b) measurements are a
46 critical component to \sqrt{s} determination as it sets the overall energy scale for
47 the collision process.

48 The strategy proposed in the International Linear Collider (ILC) design
49 [1] is to have redundant beam-based measurements capable to achieve a 10^{-4}
50 relative precision on a single beam, which would be available in real time as
51 a diagnostic tool to the operators. Also, physics reference channels such as
52 $e^+e^- \rightarrow \mu^+\mu^-\gamma$ where the muons are resonant with the known Z-mass are
53 expected to provide valuable cross-checks of the collision energy scale, but
54 only long after the data have been recorded.

55 The primary method planned to perform E_b measurements at the ILC
56 is a non-invasive beam position monitor (BPM) based energy spectrome-
57 ter similar to a setup used for calibrating the energy scale for the W-mass
58 measurement at LEP-II [2]. At the ILC, however, the parameters of the
59 spectrometer are tightly constrained to provide limited emittance dilution at
60 the highest ILC energy of 500 GeV.

61 Initially, a 3-magnet chicane located upstream of the interaction point
62 just after the energy collimators of the beam delivery system (BDS) was
63 proposed [3]. But the baseline ILC spectrometer design uses two dipole
64 magnets to produce a beam displacement x , while two more magnets return
65 the beam to the nominal beam orbit (as in fig. 1). For such a chicane, the
66 beam energy is then given by

$$E_b = \frac{c \cdot e \cdot L}{x} \int_{magnet} B dl, \quad (1)$$

67 where L is the distance between the first two magnets and $\int B dl$ the in-
 68 tegral of the magnetic field in each magnet. The 4-magnet chicane avoids
 69 spurious beam displacement signals in the BPMs due to beam tilts, and thus
 70 systematic errors in E_b measurements. For this reason, a 4-magnet spectrom-
 71 eter, which maintains the beam axially with respect to the axis of the cavity
 72 BPMs, seems preferable over a more conventional 3-magnet chicane. In both
 73 cases the magnetic field in the spectrometer chicane can be recorded and
 74 reversed for studying systematic effects without changing the beam direction
 75 downstream of the spectrometer.

76 A dispersion of 5 mm at the center of the chicane can be introduced
 77 routinely without a significant degradation of the beam emittance due to
 78 synchrotron radiation. When operating a fixed dispersion of 5 mm over the
 79 whole energy range, a BPM resolution better than $0.5 \mu\text{m}$ is needed. This
 80 resolution can be achieved with cavity BPMs [4]. Since the spectrometer
 81 bending magnets need to operate at low fields when running the ILC at
 82 the Z-pole, the magnetic field measurement may not be accurate enough
 83 to provide the required level of precision. A significantly improved BPM
 84 resolution would, however, allow the magnets to be run at the same field for
 85 both the Z-pole and highest energy operation.

86 An absolute energy measurement requires that the beam orbit measure-
 87 ment is referenced to the orbit with no field applied. Unfortunately, the
 88 residual fields still have an impact on the beam orbit at a level that may af-
 89 fect the overall beam energy accuracy. There is an ongoing R&D program to
 90 determine how to perform accurate field measurements for very low magnetic
 91 fields [5].

92 Some original energy resolution studies of the SLAC prototype 4-magnet
 93 chicane were presented by M. Viti in ref. [6]. His analysis used calibrated
 94 beam position readings but revealed that due to small differences between the
 95 magnets in the chicane the beam inclination also needs to be considered. It
 96 was soon realised that the same analysis could be extended by using complex
 97 BPM readings that contain the information on both the beam offset and
 98 inclination. This approach eliminates the need for position calibration of the
 99 BPMs, while the whole system could be calibrated by means of an energy
 100 scan.

101 In this publication we present the analysis based on that idea, estimate
102 the resolution of the spectrometer to compare it with the result of $8.5 \cdot 10^{-4}$
103 measured in [6]. We also consider the impact of different systematics on the
104 energy measurement in order to improve the resolution to below the 10^{-4}
105 level in future experiments.

106 2. Test Beam Setup and Spectrometer Hardware Configuration

107 A prototype test setup for a 4-magnet chicane was commissioned in 2006
108 (the T-474 experiment) and extended in 2007 (the T-491 experiment) in the
109 End Station A (ESA) beamline at the SLAC National Accelerator Labora-
110 tory [7].

111 In our experiments the electron beam generated by the main Linear Ac-
112 celerator at SLAC was transported to the ESA experimental area through
113 the 300 m long transfer line A including bending and focussing magnets, and
114 diagnostic instruments such as stripline and RF cavity BPMs, charge sen-
115 sitive toroids, a synchrotron light monitor, profile screens and diodes. The
116 SLAC linac was providing single bunches at 10 Hz and a nominal energy of
117 28.5 GeV, a bunch charge of $1.6 \cdot 10^{10}$ electrons, a bunch length of $500 \mu\text{m}$
118 and an energy spread of 0.15%, i.e. with beam properties similar to the ILC
119 expectations at the highest energy currently available for electrons.

120 These unique beam parameters allowed us to test the capabilities of the
121 proposed spectrometer under realistic beam conditions. Two feedback sys-
122 tems were in place for the ESA beam: one for its position and one for the
123 energy. The position feedback stabilised the beam position and angle using
124 cavity BPMs and corrector magnets upstream of the ESA area. The energy
125 feedback stabilised the energy controlling the phase of the klystrons, and
126 thus the accelerating gradient, in one of the linac sections and was also used
127 for offsetting the energy from the nominal in ± 100 MeV range.

128 The setup, as schematically shown in Fig. 1, includes four bending mag-
129 nets denoted as 3B1, 3B2, 3B3 and 3B4, forming a chicane in the horizontal
130 plane and high-precision cavity BPMs upstream, downstream and in between
131 the dipole magnets. Two of these (BPMs 4 and 7) in the middle of the chicane
132 were instrumented with precision movers. When the magnets were turned
133 on, these BPMs were mechanically moved to ensure the beam offset fits the
134 dynamic range of the BPM electronics. These movers were also used for
135 position calibrations. Horizontal positions of three monitors (BPMs 5, 4 and
136 7) were monitored with a Zygo interferometer [8].

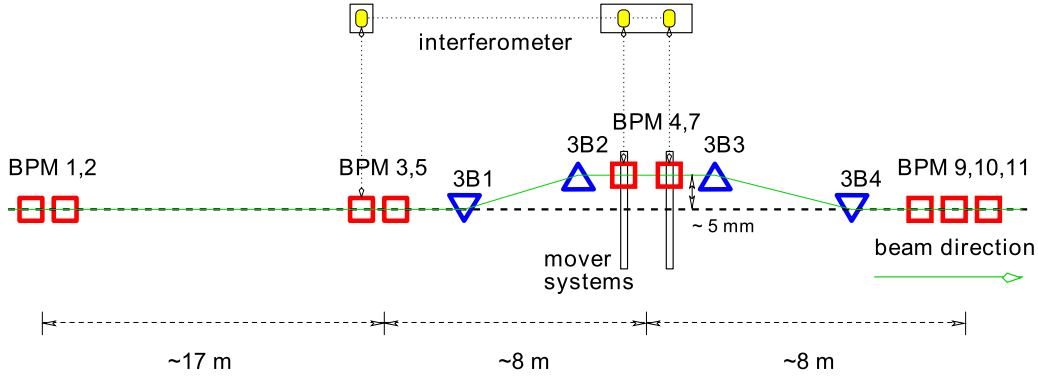


Figure 1: Schematic representation of the prototype spectrometer in ESA.

137 The 10D37 magnets from the old SPEAR injection beamline, refurbished
 138 for the use in the chicane, are 37" long, 10" wide on the pole faces and have
 139 a 3" gap. They were run in series from a single power supply to minimize
 140 relative drifts. The magnets were studied during a set of measurements in
 141 the SLAC Magnet Measurement Laboratory. Magnetic field maps of the
 142 vertical field component B_y were taken using NMR and Hall probes, while
 143 each $\int Bdl$ was measured using a flip coil, which was calibrated against a
 144 moving wire system. Stability and reproducibility were at the focus of these
 145 measurements. Details of the field measurements can be found in [6, 9, 10].

146 In situ at ESA, two NMR probes with different, but overlapping working
 147 ranges and initially also one Hall probe were installed in the first magnet
 148 3B1, while one NMR probe was positioned in each of the other three mag-
 149 nets, so that field integral values could be monitored. In the test data runs,
 150 the nominal magnetic field was 0.117 T·m which corresponds to a magnet
 151 operation at 150 A. The stray field outside the magnets in the middle of
 152 the chicane was monitored using two low-field fluxgate magnetometers. One
 153 was placed on the girder to obtain the horizontal (x) and vertical (y) field
 154 components and the other on the beam pipe measuring y -component only.
 155 Properties of the probes and the fluxgate monitors are summarized in fig. 2.

156 [discussion on NMR]

157 In order to measure the beam orbit, 8 cavity BPMs, all operating in
 158 the S-band of the RF, were installed. Three of them were SLAC prototype
 159 ILC BPMs (3, 4, 5) using cylindrical cavities with x - and y -waveguides for
 160 the dipole mode coupling and monopole mode suppression. Each of the

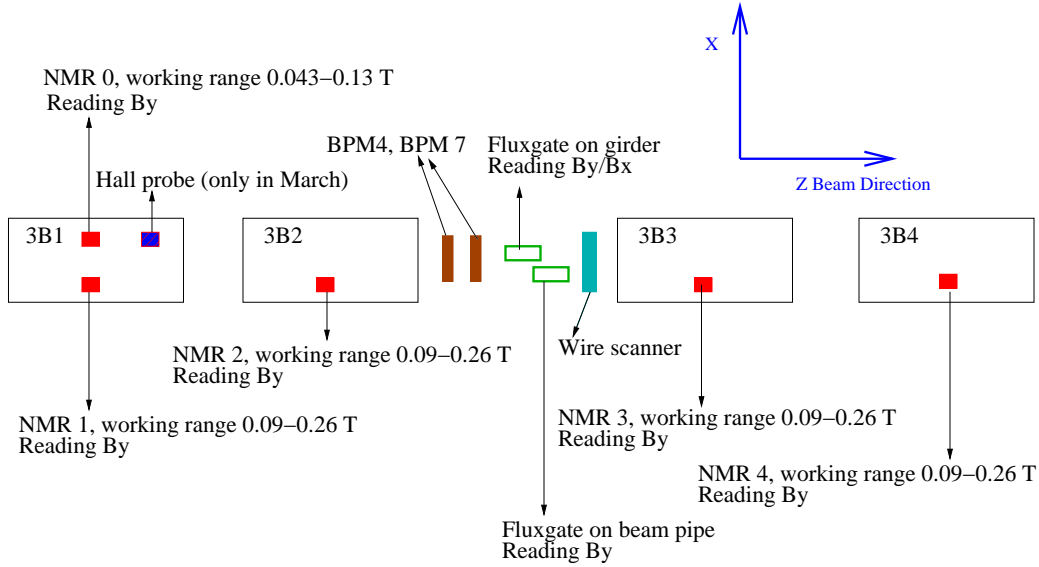


Figure 2: Magnetic field diagnostics in the spectrometer chicane.

161 five SLAC linac type BPMs (1, 2, 9, 10, and 11) consists of three cavities:
 162 two rectangular ones for x and y separately to avoid x - y couplings, and one
 163 cylindrical cavity to provide charge and phase information. BPM 7 was a
 164 dedicated ILC prototype designed and manufactured in the UK for the use
 165 in the spectrometer. Unfortunately, this monitor could not be used in the
 166 analysis due to manufacturing problems [11]. Details on the performance of
 167 the BPM system and information on the A-line configuration can be found
 168 in [4].

169 BPMs 12 and 24 are placed in the bending arc region of the A-line, where
 170 horizontal dispersion reaches several meters. For our experiment they were
 171 instrumented with the same high-sensitivity electronics as all other BPMs
 172 in the ESA beamline, so that the energy measurements in the A-line and in the
 173 chicane could be performed simultaneously and cross-checked against each
 174 other.

175 **3. Performance of the Prototype Spectrometer**

176 *3.1. Reconstruction of the beam orbit in the middle of the chicane*

177 As the chicane magnets bend the beam in the x -plane, we are mainly
178 interested in the horizontal beam position and angle, and, unless specified
179 otherwise, we talk about the x -coordinate throughout this section.

180 The offset of the beam trajectory in the middle of the chicane has to
181 be measured with respect to the nominal orbit position reconstructed using
182 BPMs outside of the chicane. In order to predict the readings of BPM 4 we
183 took data from a run with zero-current in the magnets and selected a "quiet
184 period", when neither the beam nor the hardware were manipulated. Data
185 from a run with magnets on could also be used for relative measurements
186 and would result in a better prediction, but due to the residual dispersion
187 in the beamline beam positions before and in the middle of the chicane are
188 correlated. For that reason, only data from a run with magnets off were used.

189 BPMs 9, 10 and 11 were not used for the prediction because the impact of
190 the chicane on the beam orbit when magnets are on is not fully compensated
191 due to the assymetry of the chicane, and the beam offset in these BPMs is
192 correlated with the energy.

193 Due to alignment errors, there is also a correlation between the vertical
194 beam position and angle before the chicane and the horizontal beam position
195 and angle in the mid-chicane. Therefore, both x - and y -readings from the
196 BPMs upstream of the chicane ($x_1, x_2, x_3, x_5, y_1, y_2, y_3$ and y_5) were used
197 in the analysis.

198 In our system signals generated by the BPMs were digitized and stored
199 in data files for each event, i.e. for each beam trigger. They are digitally
200 converted to the baseband in the analysis [4]. A complex digital local oscilla-
201 tor signal allows to decode both the amplitude and the phase of the signal's
202 phasor along the waveform. Sampled at a point close to the peak and nor-
203 malized by the phasor from the reference cavity, the converted waveforms
204 give the real, in-phase (I), value and the imaginary, quadrature (Q), value,
205 which contain the information on the beam offset as well as the inclination.

206 In order to reconstruct the beam orbit in the mid-chicane, the I and Q
207 values from BPM 4 are correlated to the I and Q values from the upstream
208 BPMs. We applied the Singular Value Decomposition (SVD) method [12] to
209 several thousands of readings. Inversion of the matrix of the measured I and
210 Q values for the selected BPMs provides a vector of coefficients, which relate

211 the I's and Q's of each BPM to those of BPM 4 so that a prediction can be
 212 made:

$$I_{BPM4} = \alpha_0 + \sum_i \alpha_i^{(I)} \cdot I_i + \sum_i \alpha_i^{(Q)} \cdot Q_i, \quad (2)$$

$$Q_{BPM4} = \beta_0 + \sum_i \beta_i^{(I)} \cdot I_i + \sum_i \beta_i^{(Q)} \cdot Q_i, \quad (3)$$

213 where α 's and β 's are the SVD coefficients.

214 The difference between the predicted and the measured values is called
 215 residual. In our case, the RMS residual is the precision of the orbit prediction
 216 and the resolution of BPM 4 added in quadrature. It sets the limit on the
 217 spectrometer resolution. The measured and predicted values for I and Q are
 218 plotted against each other in fig. 3. The points in these plots lie around the
 219 $y = x$ solid lines, which means the prediction works correctly. The histograms
 220 in the bottom part of fig. 3 show the residuals, for both the I and Q values.

221 It is clear that the I and Q residuals for BPM 4 are small compared
 222 to the average I and Q values, but the results in fig. 3 are still hard to
 223 interpret quantitatively. In order to set a scale we used the mover scan data.
 224 During the mover scan BPM 4 was moved in 0.25 mm steps from -0.5 to
 225 +0.5 mm off the nominal position. The precision of the mover system is
 226 about 10 μm , but the moves can also be observed by the interferometer with
 227 a sub-micrometer precision. Fig. 4 shows the scan data as well as the position
 228 residual, which was calculated for the data used in the SVD computations
 229 above. A position residual of 2.73 μm was estimated, which is close to the
 230 estimate in [6] (2.3 μm). The difference can be explained by softer applied
 231 cuts and a different minimization algorithm.

232 Assuming a 5 mm average beam offset in the middle of the chicane for
 233 magnets on, the 2.73 μm precision of the BPM system sets an energy reso-
 234 lution limit of $5.5 \cdot 10^{-4}$ for our spectrometer prototype.

235 The reader may be confused by this precision estimate comparing it to
 236 our earlier published value in ref. [4], which was close to 1 μm . This is due
 237 to the fact that BPMs 9, 10 and 11 had to be excluded from the analysis.
 238 BPM 4 used to be in the middle of the analysed system, in the "centre of
 239 gravity", while in the spectrometer studies it, unfortunately, ended up on
 240 the edge. Clearly, the precision of the orbit reconstruction at the BPM 4
 241 position was affected.

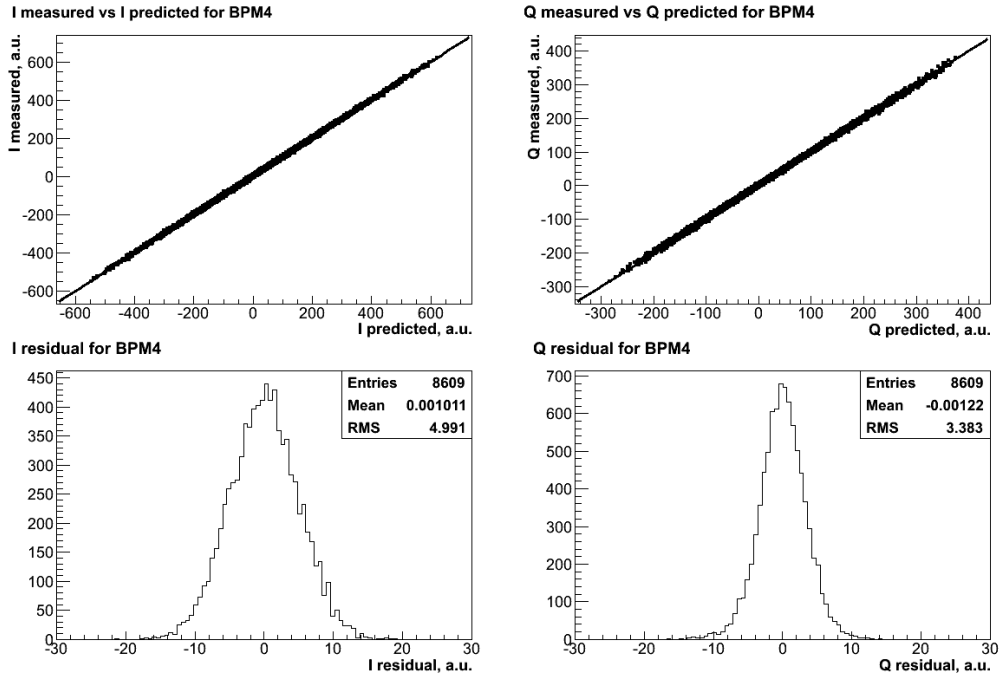


Figure 3: BPM 4 readings predicted from other BPMs in the beamline: I predicted vs I measured (top left), Q predicted vs Q measured (top right), I prediction residual (bottom left), Q prediction residual (bottom right).

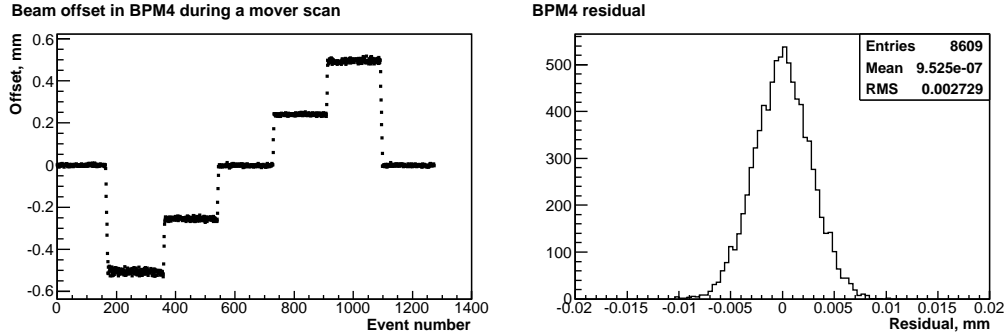


Figure 4: BPM 4 position for a horizontal mover scan (left), BPM 4 residual during a quiet period (right).

242 *3.2. Estimate of the beam energy and scale correction*

243 The I and Q readings predicted for BPM 4 by all other BPMs can be
 244 subtracted from the measured values and, when the magnets are on, provide

245 information on how the beam trajectory changes with the energy.

246 When the magnets are turned on, BPM 4 is also moved by a few mm
 247 in order to keep the beam offset within its dynamic range. This movement
 248 is observed by the precision Zygo interferometer. According to the interfer-
 249 ometer, BPM 4 was moved by 5.0034 mm between our selected runs with
 250 magnets on and magnets off. Using the IQ rotation and scale from the mover
 251 scan, we can predict the changes of the I and Q values of BPM 4. An offset
 252 of 5.0034 mm results in $I_0 = 8784$ and $Q_0 = 4605$, which were added to the I
 253 and Q values from the energy scan after the predictions had been subtracted
 254 (fig. 5, top left).

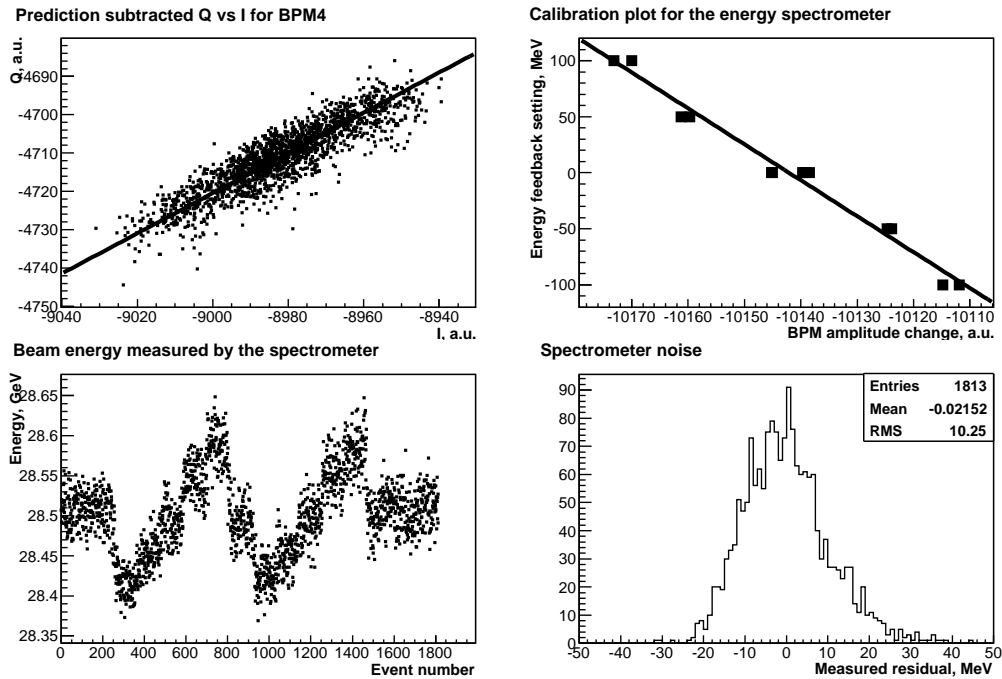


Figure 5: Beam energy measurements: prediction subtracted Q vs I for BPM 4 (offset by Q_0 and I_0 to take into account the 5.0034 mm move), the "energy line" fits the measured points (top left), energy calibration plot for the spectrometer (top right), beam energy measured during the scan (bottom left), spectrometer noise measured off the energy line (bottom right).

255 Due to small differences between the magnets a small inclination of the
 256 beam orbit is introduced along with the offset in the middle of the chicane.
 257 But the measured points in the IQ plane still lie on a straight line as both

258 the offset and inclination scale with the energy. Fitting the measured data
259 to a straight line going through the centre of coordinates, we can get the
260 IQ rotation of this "energy" line. Energy readings for each point are then
261 calculated as a projection of this point onto the energy line.

262 In order to get the energy scale, individual readings are averaged for
263 each step of the energy scan and then fitted to a straight line (fig. 5, top
264 right). The slope of this line gives the energy scale and the offset – the
265 measured nominal energy. This procedure results in a nominal energy of
266 about 32.6 GeV, while it was kept to within 1% off 28.5 GeV during the
267 run. The fit has an uncertainty of 1.4 GeV (4.3%) due to drifts during
268 the scan and prevails the total error of the measurement, but still does not
269 explain the difference. It can be attributed to the scale error of the energy
270 feedback, meaning that the energy scan was actually performed in a range
271 of $0.874 \cdot 200 \text{ MeV} = 175 \text{ MeV}$, and the energy scale factor must be corrected
272 accordingly.

273 The energy measured by BPM 4 during the scan is shown in fig. 5, bot-
274 tom left. The measured fluctuations seem to be comparable with the energy
275 scan step. In the following sections we use the data from the energy BPMs
276 in order to separate the actual energy fluctuations from noise, and also in-
277 clude additional data acquired with the setup, such as interferometer and
278 NMR readings, to refine this measurement and estimate the resolution of the
279 spectrometer.

280 The last plot in fig. 5 (bottom right) shows the distribution of the offsets
281 of the measured points from the fitted line, the RMS of the distribution
282 was estimated to 10 MeV, or $3.5 \cdot 10^{-4}$. This value is an optimistic resolution
283 estimate, as BPM readings in that plane mainly change due to the noise in the
284 BPM system. It does not include the effect of the magnetic field fluctuations
285 acting along the energy line. Indeed, our estimate using position data (sec.)
286 was $5.5 \cdot 10^{-4}$.

287 *3.3. Resolution of the energy BPMs*

288 Similarly to spectrometer data, we measured the RMS residual between
289 the fitted energy line and the measured points for the energy BPMs 12 and 24.
290 In this case we could only do a relative energy measurement, as the field of
291 the bending magnets in the A-line could not be turned off, but we were still
292 able to calibrate them using the energy scan data and take into account the
293 energy feedback scale correction.

294 The measured noise is equivalent to 0.36 MeV for BPM 12 and 2.0 MeV for
 295 BPM 24, or $1.3 \cdot 10^{-5}$ and $7.0 \cdot 10^{-5}$ respectively, at the nominal beam energy
 296 of 28.5 GeV. The values are different because BPM 12 had an additional
 297 20 dB amplifier installed in its electronics chain in order to compensate for
 298 cable losses, which improved its sensitivity and reduced the effect of the noise
 299 and granularity introduced by the digitizers.

300 Again, these estimates only take into account the noise in the BPMs,
 301 and do not take into account many other effects such as the beam jitter and
 302 the changes of the fields in the magnets. In fig. 6 we compare the energy
 303 readings of BPMs 12 and 24 after the energy calibration. An RMS residual
 304 of 4.8 MeV ($1.7 \cdot 10^{-4}$) was found, which is about twice bigger than the noise
 305 measurements combined in quadrature. This indicates that the resolution
 306 of the energy measurements of BPMs 12 and 24 is, in fact, not limited by
 307 the BPM noise alone. Nevertheless, BPMs 12 and 24 still allow for energy
 308 fluctuations to be measured to better than $1.7 \cdot 10^{-4}$, which is well below the
 309 expected spectrometer resolution.

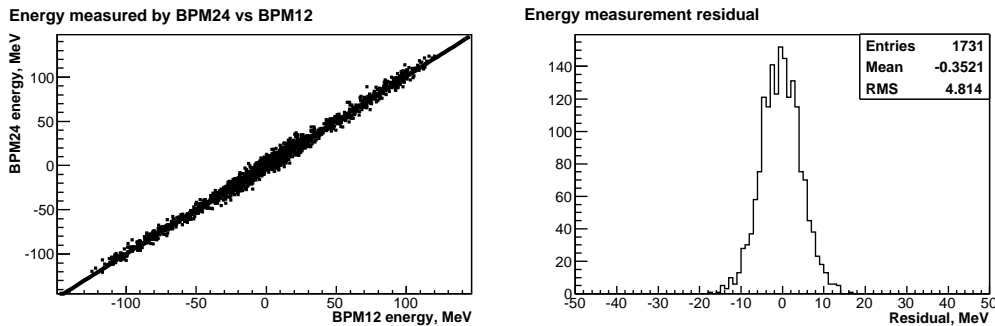


Figure 6: Comparison of BPMs 12 and 24: BPM 24 energy measurement vs BPM 12 (left), residual between BPM 12 and 24 measurements (right).

310 3.4. Dipole magnets

311 An essential prerequisite for the operation of the spectrometer in a Linear
 312 Collider is that the beam position downstream of the chicane is not energy
 313 dependant, and the upstream beam path is restored downstream. In other
 314 words, the chicane has to be symmetric. In a 4-magnet chicane it is also
 315 beneficial to match the magnets in each pair producing a parallel translation
 316 of the beam (a "dogleg"), so that the inclination of the orbit with respect to
 317 the original is kept to a minimum.

318 Magnetic field measurements were performed in March 2007 to study the
 319 response of the chicane. Some results are shown in fig. 7. Here, the differences
 320 between the measured and nominal magnetic fields are plotted as a function
 321 of the nominal value for both negative and positive polarities.

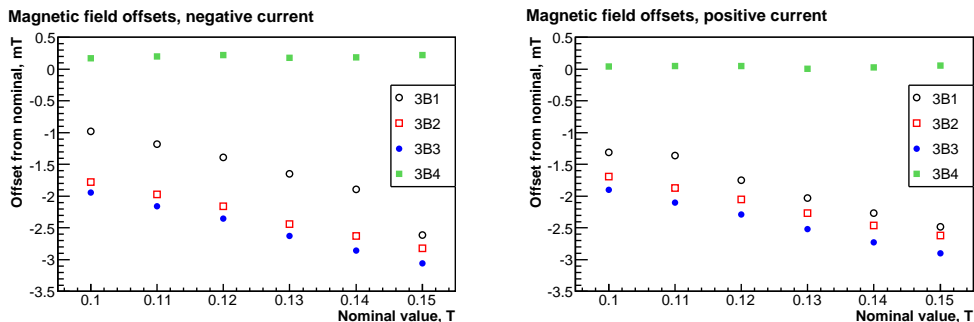


Figure 7: Offsets between the measured and nominal magnetic fields as a function of the nominal value of the four magnets in ESA: Negative current (left); Positive current (right).

322 During these measurements the field of the magnet 3B1 was monitored
 323 with a Hall probe, whereas for the other magnets NMR probes were used.
 324 As can be seen, 3B1, 3B2 and 3B3 follow the same trend, with a difference of
 325 a few tenths of a mT between 3B2 and 3B3, while 3B1 is off by about 1 mT.
 326 3B4 shows field values much closer to the nominal ones, because only for this
 327 magnet a more accurate relation between the current and the field (as given
 328 in [6]) was determined and used for the field settings. The differences in
 329 fig. 7 can be explained by the residual magnetic fields, which were estimated
 330 to be $0.2 \div 0.4$ mT (see [6]). They are expected to depend on the history of
 331 the magnets and on the properties of the core material (as the design and
 332 composition of steel cores could not be fully accounted for).

333 As a consequence, the trajectory of the beam had a small inclination
 334 in the middle of the chicane and was not fully restored downstream of the
 335 chicane, resulting in energy changes being converted into position variations
 336 in BPMs 9, 10 and 11.

337 Using the data from the upstream BPMs the nominal beam position in
 338 the downstream BPMs can be predicted. Considering, for example, BPM 9
 339 measurements after subtraction of the downstream BPMs prediction, we can
 340 clearly recognize a step-like behaviour in energy during the scan (fig. 8). Note
 341 that, although the net-integral field applied to the beam by the chicane is

342 very small, BPM 9 is still able to resolve the energy changes due to its high
 343 resolution.

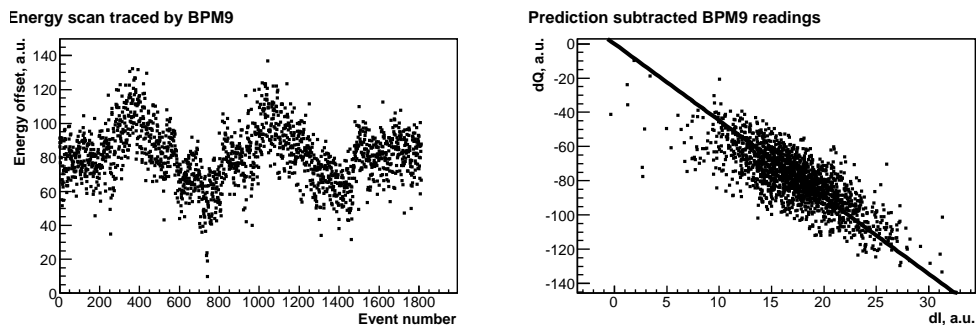


Figure 8: Energy measured by BPM 9 during the scan (left), IQ plot of the measured BPM 9 readings with the predicted readings subtracted (right). The fitted line shows the IQ rotation of the energy measurements.

344 3.5. Energy resolution of the spectrometer

345 The energy measured by the spectrometer can also be predicted by the
 346 energy BPMs 12 and 24. The residual, besides the resolutions of each BPM,
 347 depends on the fluctuations of the magnetic fields, mechanical vibrations, as
 348 well as drifts and other systematic effects and non-linearities.

349 We first compare the relative energy measured by BPM 4 with the mea-
 350 surements of BPM 12 (fig. 9, top). This results in a resolution of 24 MeV or
 351 $8.4 \cdot 10^{-4}$. As this is worse than the precision of the orbit reconstruction, we
 352 decided to look for correlations using additional data and applying the SVD
 353 method by starting again from BPM 12 (but this time the scale is corrected
 354 by SVD to better match BPM 4 readings which results to a lower residual)
 355 and then adding more data in the matrix to better reconstruct the spectrom-
 356 eter measurements and understand the systematics. Table 1 summarises the
 357 results together with the residuals calculated using the same coefficients for
 358 a quiet period when the magnets were on and nothing was changed in the
 359 system. Looking for consistent improvements of the residual, we can identify
 360 the main sources of systematic errors.

361 The biggest step in residual reduction is observed when the data from
 362 BPMs 9, 10 and 11 are included in the computation. As we know, BPMs
 363 9, 10 and 11 are sensitive to the energy, but also to the net-magnetic field

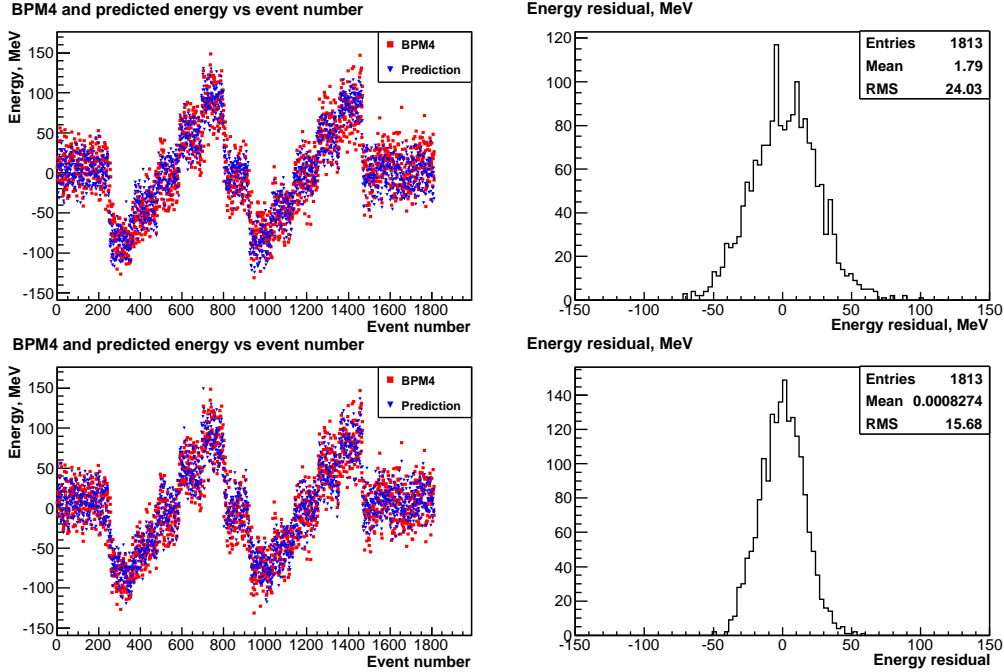


Figure 9: Energy resolution measurement: energy measured by BPM 12 and BPM 4 (top left), residual between BPM 12 and BPM 4 readings (top right), energy measurement predicted by BPMs 12, 24 and additional parameters and BPM 4 reading (bottom left), residual between the prediction and BPM 4 reading (bottom right).

364 of the chicane. Since our system did not provide bunch-to-bunch magnetic
 365 field measurements, only interpolated field data could be used. Inclusion of
 366 such data in the analysis did not provide a consistent improvement. It is
 367 therefore very likely that rapid field changes are encoded in the downstream
 368 BPM data, which might be the reason for residual improvements, when their
 369 data is added to the SVD matrix.

370 Some further improvement is also noted when the charge data, as mea-
 371 sured by one of the reference cavities, is included in the analysis, even though
 372 all the BPM data were normalised by the charge. This is best explained by
 373 the fact that BPMs 12 and 24, although very sensitive to energy changes,
 374 were not centered to their operating ranges, and were running close to satu-
 375 ration.

376 Ultimately, in order to achieve an energy resolution approaching 10^{-5} ,
 377 one has to monitor the relative motion of the BPMs in the beamline. An

Table 1: Energy residuals calculated for BPM 4 including additional parameters. $\Delta\sigma/\sigma$ is the contributed uncertainty calculated as a difference of resolutions subtraced in quadrature.

Data included	Residual, MeV		$\Delta\sigma/\sigma, \times 10^{-4}$	
	energy scan	quiet period	energy scan	quiet period
BPM 12	23.45	21.53	–	–
BPMs 12, 24	23.08	21.64	1.5	0.8 (up)
BPMs 12, 24 and NMR	22.67	22.62	1.5	2.3 (up)
BPMs 12, 24, NMR and fluxgate	22.67	22.62	–	–
BPMs 12, 24, charge (q), NMR and fluxgate	20.52	19.68	3.4	3.9
BPMs 12, 24, 9, 10, 11, q, NMR and fluxgate	15.86	15.26	4.6	4.4
BPMs 12, 24, 9, 10, 11, q, NMR, fluxgate and interferometer	15.68	14.60	0.8	1.6

378 interferometer, once well tuned, seems to be a reliable, fast and precision
379 tool. But since the mechanical vibrations observed were in the region of a
380 few hundred nanometers, the Zygo interferometer in our setup only provided
381 a moderate improvement to the energy measurement.

382 The final result of these investigations is shown in the bottom part of
383 fig. 9. With additional data included, the prediction tracks the spectrometer
384 measurement better than given in the plot above. The resolution was measured
385 to 15.7 MeV ($5.5 \cdot 10^{-4}$) for an energy scan and 14.6 MeV ($5.5 \cdot 10^{-4}$) for
386 a quiet period. These numbers are in a good agreement with the estimate
387 for the precision of the orbit reconstruction of $5.5 \cdot 10^{-4}$, which means that
388 the weighting of different systematics has been performed correctly.

389 3.6. *X to Y coupling*

390 Even though the spectrometer chicane operates in the horizontal plane,
391 the energy scan is also traced in the vertical plane. Firstly, alignment errors
392 generate a small bend in the vertical direction and, secondly, internal cross-
393 talk between the x - and y -couplers of the BPMs create spurious offset in y

394 by an offset in x .

395 In order to estimate the total cross-coupling between the x - and y -planes
396 we again consider the energy scan data in the run with magnets on, this time
397 to predict the vertical beam position in BPM 4 using the SVD coefficients
398 obtained from the run with magnets off. Clearly, as seen in fig. 10 (left), the
399 energy scan is traced in the measured y -offset. Due to different sensitivities of
400 the x - and y -channels in BPM 4, we used mover scan data in both directions
401 to get the position scale, which is used to normalise the raw energy. For that
402 reason the energy is given in terms of mm in fig. 10. One should, however,
403 keep in mind that an energy change generates both a different offset and an
404 inclination in the mid-chicane.

405 The plot on the right-hand side in fig. 10 shows the correlation between
406 the energy measured in both planes. From the inclination of the line fitting
407 the data points a rotation of BPM 4 of almost 25° is derived, or an x - y
408 isolation of about 7.6 dB. Even without tuning, BPMs usually provide an
409 isolation of 20 dB, that means the cross-talk can not be explained solely
410 by the cross-coupling of the signals. At the same time, the rotation is too
411 large to be caused entirely by the alignment errors. This indicates that both
412 effects take place. For the future, it is therefore important to minimize the
413 cross-talk in the BPMs and eliminate fake offsets by careful alignment of the
414 spectrometer elements.

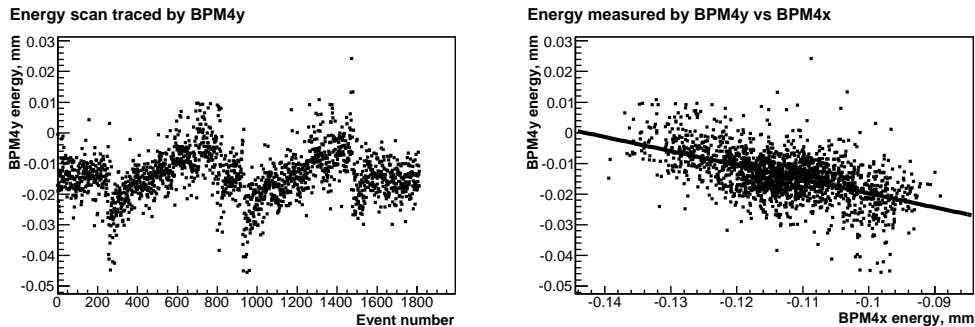


Figure 10: Effect of the chicane on the vertical beam trajectory: energy scan traced by BPM 4 in y (left), energy data measured by BPM 4 in y vs x (right). Position calibration was used to exclude the difference in sensitivities, hence, the energy is expressed in terms of the offset (mm).

415 4. Suggestions for future experiments

416 Clearly, any improvement of the BPM resolution would have a significant
417 positive impact on both the relative and absolute energy measurement as
418 it reduces the BPM uncertainties contributing to the overall measurement
419 error.

420 Improvement of the internal x - y isolation in the BPMs would also have
421 a positive impact on the energy measurement as the uncertainty introduced
422 by the signal cross-coupled from the orthogonal direction would be smaller.

423 Higher resolution BPMs could also simplify the operation of the spec-
424 trometer. For a 1 mm dispersion, a resolution of 100 nm would allow for a
425 10^{-4} energy uncertainty. Currently, a dynamic range of about 80 dB can be
426 achieved with cavity BPMs which allows a 1 mm offsets to be measured with
427 no need to move the BPMs. Hardware improvements and better algorithms
428 to treat the signals saturating the electronics [?] are expected to expand the
429 dynamic range to 90 and even 100 dB. Hence, systematic effects associated
430 with moving the BPMs to track the beam when the magnets are on can be
431 avoided without compromising the performance.

432 Without the need to move the BPMs when the chicane is in operation,
433 the BPMs are not required to be mounted on precision movers for calibration
434 purposes either, although simpler movers may still be mandatory for align-
435 ment. A direct calibration of the spectrometer can be performed by changing
436 the phase of the RF in some accelerating modules, as it was done in our ESA
437 experiment. Another way of calibration is to change the magnetic field by a
438 small but known amount and restore the energy scale from the orbit changes.

439 Working with I and Q values of the BPMs directly, we realised that even a
440 4-magnet chicane does not generate a pure beam offset in the middle because
441 of small differences between the magnets. At the required level of precision
442 the inclination still needs to be taken into account in the energy measure-
443 ments. Additional correctors after the chicane may be necessary to restore
444 the original beam orbit. Even more importantly, in a 4-magnet chicane two
445 magnets contribute to the uncertainty of the energy measurement.

446 These arguments suggest to return to the original 3-magnet chicane de-
447 sign as discussed in [3] and shown in fig. 11, where the central magnet, the
448 spectrometer magnet, is instrumented with probes and the other two help
449 to preserve the initial beam trajectory, and therefore can be controlled indi-
450 vidualy. High-precision BPMs in between the magnets provide information
451 on the bend of the beam, while BPMs upstream of the first magnet predict

452 the default trajectory downstream. In this case, the spectrometer magnet
 453 produces a combination of offset and angle in the BPMs downstream, but all
 454 measured data should still lie on one line in the IQ space as in our analysis,
 455 see section 3.2.

456 Instrumenting the ancillary magnets and extending the interferometer
 457 onto the up- and downstream BPMs would provide redundant energy mea-
 458 surement at a low increment on cost. While the overall resolution is not
 459 expected to become improved as the ancillary magnets operate at half of
 460 the B-field strength of the spectrometer magnet, some systematic effects can
 461 be a priori excluded due to the opposite bend. Furthermore, some system-
 462 atic errors can be detected because the bending angle is different (???). Also,
 463 BPM triplets instead of doublets in between the magnets would also provide
 464 redundancy of beam orbit measurements and improve both the precision and
 465 accuracy of the spectrometer. [need to explain all this?]

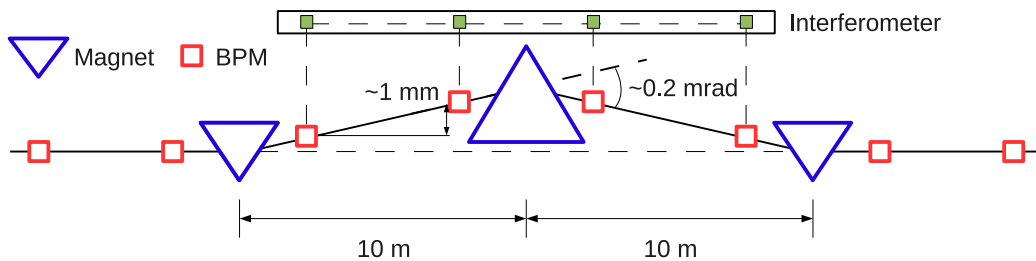


Figure 11: A 3-magnet spectrometer chicane.

466 To predict the default trajectory in a 3-magnet spectrometer, the IQ space
 467 of the BPMs can be scanned by changing the beam deflection of the ancil-
 468 lary magnets, while the spectrometer magnet is off. An additional corrector
 469 magnet downstream of the chicane may be required to fully restore the beam
 470 orbit.

471 A precision interferometer will be required to achieve the 10^{-4} or better
 472 level of precision. This becomes critical for a reduced dispersion as the BPM
 473 resolution must be enhanced to 100 nm, since RMS vibrations measured
 474 at ESA were in the order of 300 nm for stationary BPMs and approached
 475 $1 \mu\text{m}$ for BPMs mounted on the movers. The Zygo interferometer showed a
 476 precision fulfilling the spectrometer requirements, but carefully beam trigger
 477 synchronised interferometer readings must be provided.

478 The resolution of the spectrometer also depends on the availability of
479 bunch-by-bunch B-field data. The time resolution of the NMR probes is in
480 the order of tens of milliseconds, which is sufficient for bunch train averaged
481 measurements in a linear collider, but not for bunch-by-bunch operation.
482 [can we do anything?]

483 5. Summary

484 The model-independent analysis of the data obtained with the prototype
485 Linear Collider spectrometer based on a magnetic chicane revealed that a
486 resolution of $5.5 \cdot 10^{-4}$ can be achieved by means of a BPM system with mi-
487 crometer level precision for beam orbit measurements. An improved BPM
488 resolution is the key factor for enhancing the energy resolution. But to
489 achieve the 10^{-4} level, fast and reliable monitoring of the magnetic field and
490 the relative motion of the BPMs in the horizontal plane are required.

491 BPM resolutions can be pushed to the 100 nm level and below, which
492 allows to reduce the dispersion in the chicane. In this case, beam emittance
493 degradation caused by the spectrometer would be significantly reduced. Im-
494 proving the beam energy resolution even further for dynamic ranges large
495 enough to accomodate beam offsets of a milimeter would allow to operate
496 the chicane without BPM movers, and hence eliminates associated systematic
497 errors. Current analysis techniques combined with hardware improvements
498 will enhance the dynamic range of cavity BPMs beyond the current limit
499 of approximately 80 dB so that a reduced dispersion of the spectrometer is
500 possible.

501 Working with uncalibrated in-phase and quadrature BPM readings, one
502 can ignore any beam tilt from the magnets in the middle of a 4-magnet
503 chicane, as both the angle and offset follow the energy changes and the IQ
504 readings produce a straight line in the IQ space. For simplicity reasons, a
505 3-magnet chicane becomes a preferred configuration. In this case an energy
506 calibration of the whole system becomes however mandatory which could
507 replace BPM calibration. Hence, any reference to a well known physics con-
508 stant, such as the Z-mass, or a complementary method to measure E_b , is
509 important for both to correct the scale of relative measurements and to es-
510 tablish the offset for absolute energy measurements.

511 A thorough simulation of the spectrometer taking into account detailed
512 features of its components would benefit to understand the device and, possi-
513 bly, simplify the design currently proposed for the baseline of the next linear

514 collider. Once an electron test beam with suitable energy becomes available,
515 the results of the simulations should be verified in a real life environment.

516 References

- 517 [1] J. Brau, (ed.), et al., International Linear Collider reference design
518 report. 1: Executive summary. 2: Physics at the ILC. 3: Accelerator. 4:
519 Detectors ILC-REPORT-2007-001.
- 520 [2] R. Assmann, et al., Calibration of centre-of-mass energies at LEP2 for
521 a precise measurement of the W boson mass, Eur. Phys. J. C39 (2005)
522 253–292. arXiv:hep-ex/0410026.
- 523 [3] V. N. Duginov, et al., The beam energy spectrometer at the Interna-
524 tional Linear Collider, DESY LC Notes, LC-DET-2004-031.
- 525 [4] M. Slater, et al., Cavity BPM system tests for the ILC en-
526 ergy spectrometer, Nucl. Instrum. Meth. A592 (2008) 201–217.
527 doi:10.1016/j.nima.2008.04.033.
- 528 [5] N. Morozov, Progress report on developments of the magnetic field
529 measurements techniques (21-23 May respectively 21-23 November
530 2005).
531 URL [http://zms.desy.de/aktuelles/veranstaltungen_in_zeuthen/
532 konferenzen/2005/index_ger.html](http://zms.desy.de/aktuelles/veranstaltungen_in_zeuthen/konferenzen/2005/index_ger.html)
- 533 [6] M. Viti, Precise and Fast Beam Energy Measurement at the Interna-
534 tional Linear Collider, Ph.D. thesis, dESY-THESIS-2010-007 (2010).
- 535 [7] M. Hildreth, et al., Linear Collider - BPM-based energy spectrometer
536 (2004).
537 URL [http://www-project.slac.stanford.edu/ilc/testfac/ESA/
538 projects/T-474.html](http://www-project.slac.stanford.edu/ilc/testfac/ESA/projects/T-474.html)
- 539 [8] F. C. Demerest, High-Resolution, High-Speed, Low Data Age Uncer-
540 tainty Heterodyne Displacement Measuring Interferometer Electronics,
541 Meas. Sci. Technol. 9 (1998) 1024–1030.
- 542 [9] H. J. Schreiber, et al., Magnetic Measurements and Simulations of a 4
543 Magnet Dipole Chicane for the International Linear Collider Particle Ac-
544 celerator Conference PAC07 25-29 Jun 2007, Albuquerque, New Mexico.

- 545 [10] S. Kostromin, M. Viti, Magnetic Measurements for Magnets 10D37,
546 iLC-SLACESA TN-2008-1 (2008).
547 URL [http://www-project.slac.stanford.edu/ilc/testfac/ESA/
548 TechNotes/TN-2008-1.pdf](http://www-project.slac.stanford.edu/ilc/testfac/ESA/TechNotes/TN-2008-1.pdf)
- 549 [11] A. Lyapin, et al., A Prototype S-Band Cavity BPM System for the ILC
550 Energy SpectrometerEUROTeV Report 2008-072.
551 URL http://www.eurotev.org/reports_presentations/eurotev_reports/2008/e1526/E
- 552 [12] W. H. Press, et al., Numerical Recipes in C, Cambridge University
553 Press, 1992.